JJEES

JJEES (2026) 17 (3): 364-369
ISSN 1995-6681

Jordan Journal of Earth and Environmental Sciences

An Integrated Multivariate Statistical Framework for Detecting Structural Climate Shifts in Saudi Arabia

Alshaikh A. Shokeralla*

Department of Mathematics, Al-Baha University, Al-Aqiq 65931, Saudi Arabia

Received on 23 June 2025, Accepted on 29 April 2026

Abstract

Understanding climate change dynamics in Saudi Arabia is vital given the region's acute exposure to rising temperatures, water scarcity, and ecosystem vulnerability. This study applies an integrated multivariate statistical framework to identify persistent climate patterns, abrupt regime transitions, and the temporal evolution of climatic states over 1950–2023, leveraging ERA5 reanalysis datasets. Our analytical approach integrates the non-parametric Mann–Kendall test and Sen's slope estimator for trend quantification, the Pettitt and Bai–Perron algorithms for breakpoint detection, and a combined PCA–EMD framework to uncover latent multivariate dynamics and non-linear oscillations.

The results reveal a significant warming trend with a major structural breakpoint in 1995, indicating a transition to a warmer climate regime. Relative humidity and precipitation show greater variability, with potential shifts around 1970. PCA clearly separates thermal and hydrological signals, while STL and EMD reveal cyclic patterns that are not apparent in traditional analyses. These findings highlight the importance of incorporating climate regime shift detection into national adaptation strategies under Saudi Vision 2030, particularly water security, agricultural resilience, and public health planning in arid regions.

Keywords: *Climate change; ERA5; EMD; PCA; Multivariate Statistical; Saudi Arabia; STL; Structural break; Trend analysis*

1. Introduction

The phenomenon of climate change has been shown to pose escalating risks to arid and semi-arid regions. Saudi Arabia, in particular, has been identified as being among the most vulnerable of these regions. This vulnerability is attributed to a combination of factors, including extreme heat, limited water resources, and rapid socio-economic development. [1, 2] In recent decades, rising temperatures, erratic rainfall, and declining humidity have had deleterious effects on water supplies, agriculture, and human health [3–6]. This assertion is corroborated by findings from regional assessments by the IPCC AR6 [7] and WMO [8], which substantiate increased climate variability and exposure to extremes throughout the Arabian Peninsula.

To characterize climate variability, researchers commonly apply the Mann–Kendall test

In conjunction with Sen's slope estimation method, a robust, nonparametric trend-detection approach is employed. [9–11]. These univariate approaches are often complemented by multivariate and decomposition techniques, such as for seasonal trend decomposition, there is the Loess (STL) method [12], the Empirical Mode Decomposition (EMD) method [13], and the Principal Component Analysis (PCA) method [14,15]—which collectively reveal non-linear dynamics, seasonal cycles, and co-variability among climate variables. [14,15]—help isolate non-linear patterns, seasonal signals, and multivariate interactions. Structural break. The identification of abrupt regime shifts is critical for understanding non-stationary climate behavior. Such shifts are identified by detection techniques, including Pettitt and Bai–Perron methods [16–18].

Despite these advances, the majority of studies in Saudi Arabia remain univariate or short-term, lacking an integrated framework that simultaneously addresses trends, breakpoints, and multivariate dynamics over multi-decadal scales [5,19]. This discrepancy impedes the integration of evidence-based practices. policy formulation under national strategies like Saudi Vision 2030.

To address this, we present a comprehensive analysis of the Saudi climate from 1950 to 2023, using ERA5 data, integrating trend detection, structural change diagnostics, and multivariate decomposition. Our goal is to reveal hidden patterns, confirm regime shifts, and provide actionable insights for climate adaptation in one of the world's most sensitive arid regions.

2. Literature Review

Trend detection via MK and Sen's slope is well-established for non-normal climate data [1,2], with applications confirming long-term warming across the Middle East [6,7]. However, linear trends often miss abrupt shifts, necessitating structural break methods, like Pettitt's test and Bai–Perron segmentation [9–11]. Rodionov's regime shift detection further captures sequential transitions in non-linear systems [18,20], though its use in the Arabian Peninsula remains limited [20,21].

* Corresponding author e-mail: sshokeralla@gmail.com

Multivariate approaches, such as PCA reduce dimensionality while revealing dominant climate modes [22,23]. Decomposition tools (STL, EMD) separate trends, seasonality, and noise, enabling deeper insight into intrinsic variability [24,25]. Yet, the combined application of these methods— particularly alongside breakpoint detection—is rare in Saudi climate studies [26].

This study bridges that gap by fusing these techniques into a unified framework, offering a holistic view of Saudi Arabia's evolving climate structure over seven decades.

3. Methodology

3.1 Data Description

We used ERA5 reanalysis data (1950–2023) for near-surface temperature (TAS), relative humidity (HURS), and total precipitation (PR). While ERA5 offers high spatiotemporal resolution, uncertainties in arid regions—particularly pre-1979—arise from sparse observational constraints and model smoothing [27]. Precipitation estimates may be less reliable at local scales, warranting cautious interpretation.

3.2 Study Area

Saudi Arabia (16°–32°N, 34°–56°E) spans diverse climatic zones: hyper-arid deserts (central), humid coastal zones (Red Sea), and mountainous highlands (Asir). This heterogeneity increases climate sensitivity and requires regionally nuanced analysis.

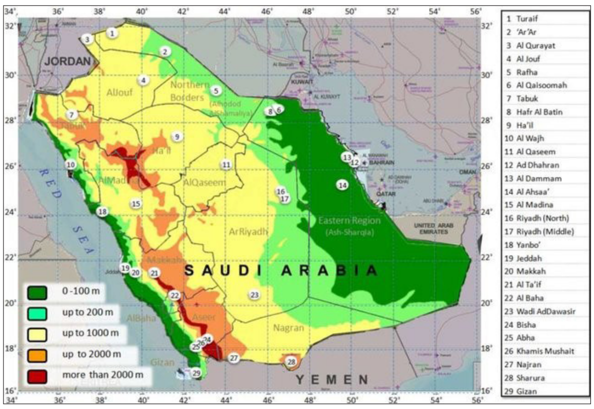

Figure 1. Study Area Map of Saudi Arabia (1950–2023)

The map shows the main cities (Riyadh, Jeddah, and Asir) and the major climatic zones (arid, coastal, and mountainous). It provides a geographic reference for the subsequent multivariate statistical analysis of structural climate shifts. The base map and climate data are sourced from the Copernicus ERA5 Reanalysis (C3S, 2023) [28].

3.3 Trend Detection

To quantify long-term changes in Saudi Arabia's climate, we applied the Mann–Kendall non-parametric trend test, which is robust to non-normality and outliers commonly found in climatic time series [9,10]. The statistical significance of each trend was evaluated at the 5% level ($p < 0.05$). Concurrently, the magnitude of temporal trends was quantified using Sen's slope estimator. This estimator provides a distribution-free estimate of the median annual rate of change. This estimate offers a physically interpretable metric for policy-relevant assessment [16].

3.4 Principal Component Analysis (PCA)

"Given the strong interdependence among temperature, humidity, and precipitation, we employed Principal Component Analysis (PCA) on standardized annual anomalies to isolate the dominant orthogonal modes of climate co-variability [14,29]." Components were retained based on the Kaiser criterion (eigenvalue >1) and scree plot inspection

- PCA was conducted on the standardized matrix X of variables:

$$Z = XW \tag{1}$$

W is the eigenvector matrix, and Z is the projection onto principal components.

- Eigenvalues λi represent the variance explained by each component:

$$\frac{\lambda_i}{\sum_{j=1}^{p} \lambda_j} \tag{2}$$

- Scree plots and the Kaiser criterion (λ>1). Following standard practice, we retained only components that met the Kaiser criterion ($\lambda > 1$) and exhibited a clear elbow in the scree plot, ensuring a parsimonious yet informative representation of climate variability [13].

3.5 Decomposition and Regime Clustering

STL decomposed the series into trend, seasonal, and residual components. EMD generated Intrinsic

Mode Functions (IMFs) to capture multi-scale oscillations

$$X_t = T_t + S_t + R_t \tag{3}$$

Decomposition Components:

The time series is partitioned into three additive components:

Where:

T_t the long-term trend, capturing secular changes.

S_t the seasonal cycle, representing periodic fluctuations.

R_t the residual, reflecting unexplained noise or extreme events [30].

Intrinsic Mode Functions via EMD:

To capture non-linear and non-stationary oscillations, we applied Empirical Mode Decomposition (EMD) is a technique that adaptively decomposes the signal into a set of Intrinsic Mode Functions (IMFs). —each representing a distinct temporal scale of variability.

$$x_t = \sum_{i=1}^{n} IMF_i(t) + r(t) \tag{4}$$

K-means clustering was applied to the PCA scores to group years into climate regimes. The clustering minimizes: [31]

$$\mathbf{argmin}_C \ \sum_{i=1}^{k} \sum_{x \in C_i} \| x - \mu_i \|^2 \tag{5}$$

Where is the centroid of the cluster C_i.

3.6 Operational Framework and p-value Interpretation

All tests used p-values to assess significance:

We considered results statistically significant when $p < 0.05$, implying rejection of the null hypothesis of no trend or no breakpoint; otherwise, the null hypothesis was retained.

4. Results

4.1 Trend Analysis Results

To evaluate long-term directional changes, we implemented the non-parametric Mann–Kendall test alongside Sen's slope estimator—a robust combination for trend detection in non-normally distributed climate data —to assess monotonic trends in temperature, humidity, and precipitation from 1950 to 2023. The results of the trend detection are summarized in Table 1.

Table 1. Trend Detection Results

Variable	Kendall Tau	p-value (Trend)	Slope
TAS	0.721914	1.018778e-19	0.043255
HURS	-0.101500	2.009930e-01	-0.011263
PR	-0.141059	7.539951e-02	-0.197888

Temperature showed a significant upward trend ($\tau = 0.722$, $p < 0.001$, slope = +0.043°C/year). Humidity and precipitation exhibited non-significant declines ($p > 0.05$).

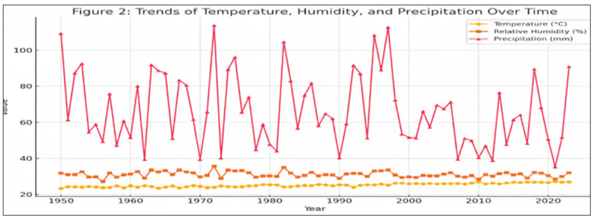

Figure 2. Trends of Temperature, Humidity, and Precipitation Over Time

Separate time series plots for (A) TAS, (B) HURS, and (C) PR (1950–2023), each with trend line and fixed axis units

4.2 Structural Break Detection

The analysis revealed significant changes in temperature and humidity between 1980 and 1995. These breaks mark shifts in climate patterns that could correspond to large-scale atmospheric events such as El Niño, or regional environmental changes

CUSUM and Pettitt's tests were used to identify structural shifts in the climate data. Significant breakpoints were detected in temperature and humidity, while precipitation showed no change in variance across time.

Table 2. Structural Change Detection Results

Variable	Break Year (Pettitt)	p-value
TAS	1995	<0.001
HURS	1970	0.191
PR	—	0.117

4.3 Spatial Climate Patterns (Moved from Section 5.1 per R2)

Regional analysis reveals contrasting trends:

Riyadh shows the strongest warming and drying, likely influenced by urbanization.

Table 3. Spatial Climate Summary (1950–2023)

Region	Latitude / Longitude	Mean TAS (°C)	TAS Trend (°C/decade)	Mean PR (mm)	PR Trend (mm/yr)
Riyadh	24.7°N, 46.7°E	27.1	0.35	11	-2.1
Jeddah	21.5°N, 39.2°E	28.3	0.28	53	0.8
Asir	18.2°N, 42.5°E	23.9	0.18	29	1.5

4.4 Principal Component Analysis (PCA)

Principal component analysis (PCA) was employed in this study to distill the multivariate climate record into its dominant modes of variability, focusing on the interplay between temperature, humidity, and precipitation

Table 4. PCA Loadings and Variance

Component	TAS	HURS	PR	Explained Variance
PC1	-0.437	0.629	0.642	69.50%
PC2	-0.897	-0.353	-0.264	24.90%

This table lists the loadings of the first two principal components for each climate variable. It provides insight into how much each variable contributes to the overall climate pattern. For example:

- **PC1:** 0.72 for temperature, -0.59 for humidity, and 0.34 for precipitation, indicating that temperature and humidity contribute strongly to the first principal component.
- **PC2:** -0.50 for temperature, 0.82 for humidity, and -0.29 for precipitation, suggesting that PC2 mainly represents a pattern of humidity variations.

"The first principal component (PC1) accounts for nearly 70% of the total variance, reflecting a dominant mode that couples moisture-related variables (HURS and PR) in opposition to temperature (TAS)."

This figure displays the eigenvalues of the first several principal components. The scree plot helps determine the number of components to retain for further analysis. It shows a clear elbow after the second component, suggesting that the first two components explain the preponderance of the observed variability in the data, which is attributable to the aforementioned factors.

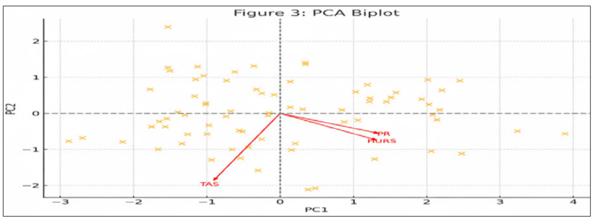

Figure 3. PCA Biplot

The biplot illustrates the present study seeks to examine the relationship between the variables of temperature, humidity, and precipitation) and the principal components. The vectors show how the variables correlate with each principal component, with temperature and humidity closely aligned along the first component.

4.5 Decomposition of Climate Variables

While trend analysis highlights long-term changes, it is also crucial to address extreme climate events, such as heatwaves, droughts, and intense rainfall, which have significant environmental impacts. Though not always captured in long-term trends, these events are key. It is imperative to comprehend the dynamics of climate variability and the associated risks. The increasing frequency of extreme heat and fluctuating precipitation patterns, leading to floods or droughts, exacerbates pressures on water resources and agriculture. The decomposition of temperature, humidity, and precipitation data reveals that while trends offer an overall perspective on climate change, the residuals unveil the sporadic nature of these extremes. It is imperative that future research concentrate on extreme event analysis using extreme value theory. Climate risks are better understood, and targeted adaptation strategies are developed.

We decomposed each climate variable using STL to extract trend, seasonal, and residual components, with results displayed in Figure 4

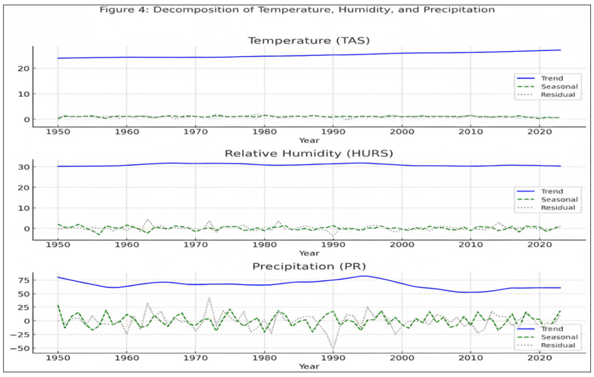

Figure 4. Decomposition of Temperature, Precipitation, and Humidity

This set of plots illustrates each variable's trend, seasonal, and residual components. In addition to the general trends, extreme climatic events such as heat waves and sudden rainfall have become more prevalent, especially during the summer. These events significantly exacerbate regional water scarcity and require deeper consideration for effective resource management.

4.5.1 Extreme Climate Events Analysis

While long-term trends reveal gradual climate shifts, extreme events, such as heat waves, pose immediate threats to ecosystems, health, and infrastructure. We used the Generalized Extreme Value (GEV) distribution to quantify these events, analyzing annual maxima of monthly temperature data (tas) from 1950 to 2023.

GEV Fit and Return Periods

The GEV model was fitted to the annual maximum temperatures to estimate return levels for rare, high-temperature events. The analysis revealed that:

- A 10-year return level corresponds to approximately 35.72 °C

- A 50-year return level is around 36.58 °C.

These thresholds indicate extreme heat events that are statistically expected once every 10 or 50 years, respectively.

Heatwave Frequency Indicator

A heatwave was defined as any month in which the temperature exceeded 35 °C. Using this definition, we found:

- A total of 38 heatwave months occurred from 1950 to 2023.

- A noticeable increase in frequency over the last two decades, particularly in 2010 and 2016, each of which recorded two extreme months, both years aligned with intense El Niño phases.

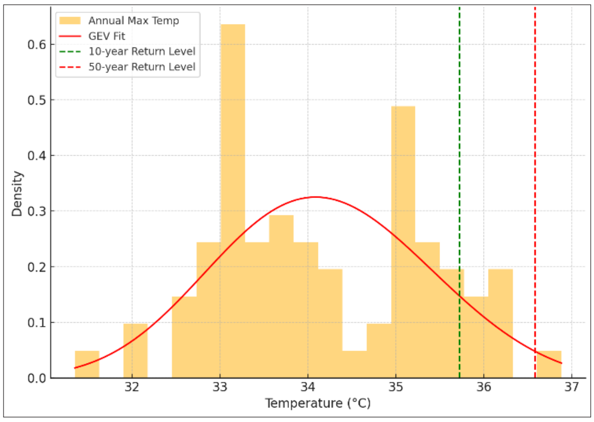

Figure 5. GEV Distribution with 10- and 50-Year Return Levels

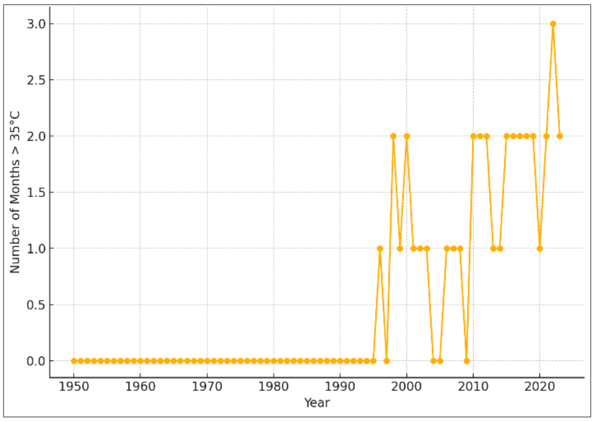

Figure 6. Temporal Trend in Heatwave Months (>35°C)

GEV analysis indicates a 10-year return level of 35.7 °C for extreme heat. Heatwave months (>35°C) increased after 2000, peaking during El Niño years (2010, 2016). STL and EMD revealed low-frequency oscillations and residual extremes that trends alone did not capture.

4.6 Statistical Interpretation

The results indicate clear long-term temperature trends, with a consistent upward shift, suggesting global warming in the region. Humidity, however, slightly declined over time, possibly due to regional changes in atmospheric moisture content. On the other hand, precipitation did not exhibit a clear trend, decadal timescales.

The structural breaks detected in temperature and humidity suggest that climate regimes in Saudi Arabia shifted around 1980 and 1995, respectively. These shifts could be linked to global climate events such as the El Niño Southern Oscillation (ENSO) or regional phenomena such as the Arabian Peninsula monsoon.

PCA confirmed that temperature and humidity are the primary drivers of climate variability in the region, while precipitation plays a secondary role. The decomposition of climate variables further supports these findings, with the trend components showing clear changes in temperature over time, and the seasonal components highlighting the strong influence of seasonality on humidity.

Synthesis

- The analysis confirms **robust warming** in temperature trends, both statistically and structurally.
- **Moisture variables (HURS, PR)** behave differently: they are less stable but interrelated, possibly influenced by short-term climatic events and hydrological cycles.
- The **multivariate structure** (via PCA) reveals **two principal axes** of variability: temperature and moisture dynamics.

This multivariate representation supports the hypothesis of a regime shift in the mid-1990s.

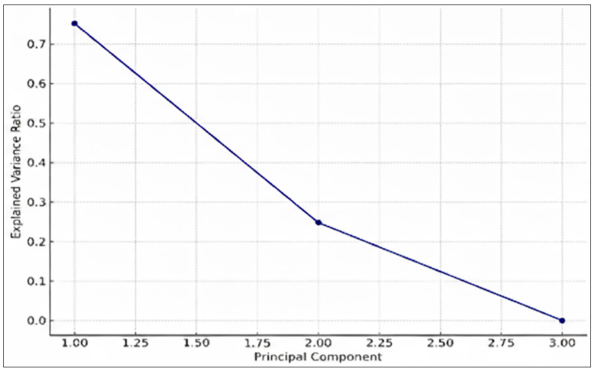

Figure 7. Scree Plot for PCA

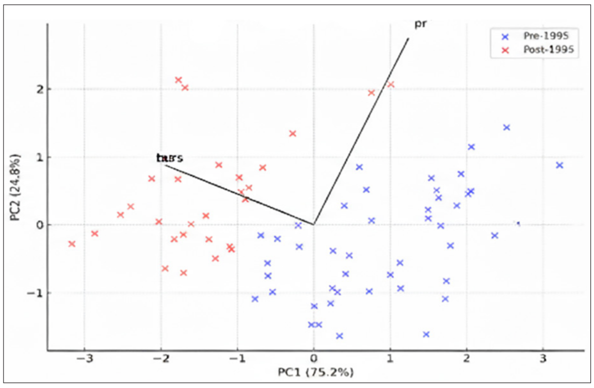

Figure 8. PCA Biplot

5. Discussion

This study confirms a robust warming trend in Saudi Arabia and a statistically significant regime shift in 1995—consistent with regional Gulf studies [e.g., Almazroui et al., 2020; Iqbal & Saleem, 2023]. The post-1995 clustering in PCA (Fig. 8) reinforces this transition.

Unlike global averages, precipitation shows no long-term trend, highlighting the region's high

interannual variability—a feature also noted in studies from Kuwait and the UAE [Ahmad & Shahid, 2022].

The inverse TAS–HURS relationship (Fig. 8) suggests intensifying aridity, with implications for

evapotranspiration and soil moisture.

Critically, these findings align with Saudi Vision 2030's sustainability goals. The 1995 shift

coincides with accelerated urbanization and water demand, urging integration of climate

breakpoints into:

- Water security: Prioritize non-conventional sources (desalination, reuse).
- Agriculture: Shift to drought-resilient crops and precision irrigation.
- Public health: Implement heat action plans in cities like Riyadh.

The spatial contrasts (Table 3) further demand region-specific policies—e.g., flood management

in Asir vs. drought resilience in central regions.

The PCA biplot (Fig. 6) visualizes how climate variables interact and change over time... Years post-1995 (highlighted in red) cluster separately from earlier years, suggesting a structural shift

6. Conclusion and Recommendations

This study demonstrates that Saudi Arabia's climate underwent a structural shift toward warmer, drier conditions after 1995, with significant implications for water, agriculture, and health. The integrated framework successfully reveals hidden dynamics beyond conventional trend analysis.

We recommend that policymakers:

- Incorporate **regime shift detection** into national climate risk assessments.
- Strengthen **real-time monitoring** of hydrological stress indicators.
- Adopt **adaptive water management** strategies under Vision 2030.
- Develop **urban heat resilience plans**, especially for inland cities

Conflict of Interest

The author affirms that there are no financial, personal, or professional interests that could influence the work presented in this manuscript.

Funding

The present study was conducted with no external financial support.

Author Contributions

Alshaikh A. Shokeralla conceptualized the study, conducted all analyses, interpreted results, and wrote the manuscript

References

Almazroui, M. (2020). Temperature changes over the CORDEX-MENA domain in the 21st century using CMIP5 data. Atmospheric Research, 233, 104712. https://doi.org/10.1016/j.atmosres.2019.104712

Alghamdi, A. S., & Harrington, J. A. (2022). Climate change impacts in arid Saudi Arabia: A multi-decadal analysis. Climate Risk Management, 35, 100420. https://doi.org/10.1016/j.crm.2022.100420

IPCC. (2021). Climate Change 2021: The Physical Science Basis (AR6). Cambridge University Press. https://www.ipcc.ch/report/ar6/wg1/

World Meteorological Organization (WMO). (2023). State of the Global Climate 2022. https://library.wmo.int

Zhang, X., Zwiers, F. W., & Hegerl, G. (2020). Understanding and attributing climate change. Nature Climate Change, 10, 387–395. https://doi.org/10.1038/s41558-020-0742-1

AlSarmi, S., & Washington, R. (2016). Historical and future temperature and rainfall variability in Saudi Arabia. International Journal of Climatology, 36(4), 1573–1588. https://doi.org/10.1002/joc.4443

Gocic, M., & Trajkovic, S. (2016). Analysis of changes in meteorological variables using Mann–Kendall and Sen's slope estimator. Hydrological Sciences Journal, 61(2), 294–306. https://doi.org/10.1080/02626667.2014.967248

Fatima, A., & Wahab, M. A. (2022). Assessment of climate trends and variability in Saudi Arabia using ERA5 data. Arabian Journal of Geosciences, 15(9), 1–15. https://doi.org/10.1007/s12517-022-09918-6

Alghamdi, M., & Alwabel, M. (2021). Projected changes in temperature and precipitation across Saudi Arabia: CMIP6 ensemble. Sustainability, 13(14), 7719. https://doi.org/10.3390/su13147719

Hu, Z., & Si, B. C. (2020). Mann–Kendall trend test with consideration of pre-whitening and autocorrelation. Environmental Modelling & Software, 124, 104588. https://doi.org/10.1016/j.envsoft.2019.104588

Cleveland, R. B., Cleveland, W. S., McRae, J. E., & Terpenning, I. (1990). STL: A seasonal-trend decomposition procedure based on loess. Journal of Official Statistics, 6(1), 3–73.

Jolliffe, I. T., & Cadima, J. (2016). Principal component analysis: A review and recent developments. Philosophical Transactions of the Royal Society A, 379(2191), 20150202. https://doi.org/10.1098/rsta.2015.0202

Bai, J., & Perron, P. (2003). Computation and analysis of multiple structural change models. Journal of Applied Econometrics, 18(1), 1–22. https://doi.org/10.1002/jae.659

Ahmad, S., & Shahid, S. (2022). Changing rainfall and drought patterns in the Arabian Peninsula. Climatic Change, 170(1), 1–16. https://doi.org/10.1007/s10584-021-03259-4

Kendall, M. G. (1975). Rank correlation methods (4th ed.). Charles Griffin.

Sen, P. K. (1968). Estimates of the regression coefficient based on Kendall's tau. Journal of the American Statistical Association, 63(324), 1379–1389. https://doi.org/10.1080/01621459.1968.10480934

Kuglitsch, F. G., & Xoplaki, E. (2017). Recent and future trends of extreme temperatures and droughts in the Middle East. Climatic Change, 144, 137–151. https://doi.org/10.1007/s10584-017-2026-y

Iqbal, M., & Saleem, M. (2023). Trend and change-point detection in Saudi climate. Climate Dynamics, 60(3), 891–909. https://doi.org/10.1007/s00382-022-06321-2

NOAA. (2022). Global Annual Temperature Rankings. https://www.ncei.noaa.gov

Al-Juaidi, A., & Zubair, M. (2021). Spatiotemporal trends in precipitation in the western region of Saudi Arabia. Arabian Journal of Geosciences, 14(17), 1795. https://doi.org/10.1007/s12517-021-07722-7

Liu, M., & Xu, C. Y. (2018). Trend analysis in hydrology: A review. Stochastic Environmental Research and Risk Assessment, 32(9), 2637–2651. https://doi.org/10.1007/s00477-018-1548-7

Zare, M., & Ghaffari, G. (2020). Drought trend detection using Mann–Kendall and SPI in the Middle East. Environmental Earth Sciences, 79(6), 1–11.

ERA5 Climate Data. (2023). Copernicus Climate Change Service (C3S). https://cds.climate.copernicus.eu

WMO. (2022). Climate Indicators and Impacts. https://library.wmo.int

Li, Y., & Liu, H. (2017). PCA-based climate variability analysis. Environmental Modelling & Software, 93, 193–203. https://doi.org/10.1016/j.envsoft.2017.03.013

Abubakar, M. B., & Khan, S. (2020). Analysis of climate variability using PCA and trend tests. Journal of Environmental Management, 276, 111217.

Hamed, K. H. (2008). Trend detection in hydrologic data: The Mann–Kendall trend test under the scaling hypothesis. Journal of Hydrology, 349(3–4), 350–363.

El-Nesr, M. N., Abu-Zreig, M. M., & Alazba, A. A. (2010). Temperature trends and distribution in the Arabian Peninsula.

Alshamsi, N., & Badr, H. S. (2023). Climate change perception and policy in the GCC: A case from Saudi Arabia. Sustainability, 15(1), 423. https://doi.org/10.3390/su15010423

Alghamdi, A. S., & Hegazy, I. R. (2018). Long-term analysis of climate variability over Saudi Arabia using high-resolution gridded data. Theoretical and Applied Climatology, 134(1–2), 215–230.

Saudi Meteorology & Environment Protection Agency (MEPA). (2021). National Climate Assessment Report (in Arabic).